Synthesis, Biological Evaluation, and Molecular Docking of Ugi Products Containing a Zinc-Chelating Moiety as Novel Inhibitors of Histone Deacetylases

Ambra A. Grolla,[†] Valeria Podestà,[†] Maria Giovanna Chini,[‡] Simone Di Micco,[‡] Antonella Vallario,[†] Armando A. Genazzani,[†] Pier Luigi Canonico,[†] Giuseppe Bifulco,*[,‡] Gian Cesare Tron,[†] Giovanni Sorba,[†] and Tracey Pirali*[,†]

Dipartimento di Scienze Chimiche, Alimentari, Farmaceutiche e Farmacologiche and Drug and Food Biotechnology Center, Università degli Studi del Piemonte Orientale "A. Avogadro", Via Bovio 6, 28100 Novara, Italy, and Dipartimento di Scienze Farmaceutiche, Università di Salerno, via Ponte Don Melillo, 84084 Fisciano (SA), Italy

Received December 4, 2008

HDAC inhibitors show great promise for the treatment of cancer. As part of a broader effort to explore the SAR of HDAC inhibitors, synthesis, biological evaluation, and molecular docking of novel Ugi products containing a zinc-chelating moiety are presented. One compound shows improved inhibitory potencies compared to SAHA, demonstrating that hindered lipophilic residues grafted on the peptide scaffold of the α-aminoacylamides can be favorable in the interaction with the enzyme.

Introduction

HDACs[a] have a key role in the epigenetic regulation of gene expression.[1] HDACs have been divided into two distinct classes, operating by a zinc-dependent (class I/II/IV) or a NAD-dependent (class III) mechanism. These enzymes catalyze the removal of acetyl groups from lysine residues on proteins, including histones. Because aberrant histone acetylation has been linked to malignant diseases, HDAC inhibitors bear great potential as new antitumor drugs; indeed, they can induce differentiation, growth arrest, and apoptosis in transformed cell cultures. Many of these agents are effective in the inhibition of tumor growth in vivo and some have entered clinical trials as possible antitumor agents.[2] In October 2006, the FDA approved the first HDAC inhibitor, SAHA, to treat cutaneous T-cell lymphoma.[3] Despite the variety of structural characteristics, most HDAC inhibitors can be broadly described by a common pharmacophore fitting the HDAC tubular pocket. This pharmacophore includes a cap group, which makes contacts with the residues on the rim of the enzymatic active site, and a zinc-chelating moiety, joined by a linker domain which occupies the hydrophobic tunnel.[4]

CHAP 1 (**1**) is a trapoxin B analogue in which epoxyketone is replaced with hydroxamate, leading to a compound that reversibly inhibits HDAC at nanomolar concentrations, with a superior in vivo stability compared to trapoxin B.[5] In a SAR study on CHAP derivatives it has been shown that the presence of two hydrophobic amino acids, such as the bis-phenylalanine moiety, is fundamental for the interaction with two lipophilic binding sites of HDACs.[6] With the aim of probing binding interactions on the outer rim of HDAC enzymes, we decided to focus on the bis-phenylalanine region markedly simplifying **1**, generating a diamide scaffold by an Ugi reaction (Chart 1).[7] This led to a peptidomimetic structure displaying a tertiary amide, making it possible to investigate the role of an additional substituent (R_3). Furthermore, we also investigated different side chains (R_1, R_2), analyzing their influence on HDAC activity.

Chemistry

With this strategy in mind, different building blocks (isocyanides, **2**−**4**, aldehydes, **5**−**8**, amines, **10** and **11**, and carboxylic acids containing the alkyl chain and a methyl ester, **12** and **13**) were chosen (Figure 1).

The key reaction in the synthesis of the proposed HDACs inhibitors is the Ugi reaction, which leads to the α-aminoacylamide displaying an ester function. The methyl ester is then transformed into the corresponding hydroxamate passing through the carboxylic acid intermediate (Scheme 1). The Ugi reaction was performed in classical conditions (MeOH, 2 M, 48 h, r.t.), leading to the α-aminoacylamides in moderate yields (17−44%). Several attempts to optimize the transformation (**2**, **9**, **5**, **12**) were made; in detail, temperature (reflux), solvent (trifluoroethanol), reaction times (up to 7 days), and molar ratios (excess of **9** and **5**) were varied, alongside preforming the imine intermediate. Yet, none of these strategies proved better, in respect to the presence of starting materials, byproduct, and yields of the desired product.

The hydrolysis of the methyl esters (**14**−**22**) to the corresponding carboxylic acids (**23**−**31**) was performed with LiOH in THF/water. The hydroxamic acids (**32**−**40**) were prepared by subsequent reaction with TBDMS-protected hydroxylamine, EDCI, and TEA in CH_2Cl_2, and final deprotection with TBAF in THF.

To probe the structure−activity relationship of the metal-chelating group, we also synthesized analogues of **32** and **39**, replacing the hydroxamates with benzamides. Benzamides were synthesized (**41** and **42**), coupling the corresponding carboxylic acids to *o*-phenylenediamine using standard peptide chemistry (DCC in THF; Scheme 2).

Biological Results

To test the activity of the synthesized compounds, we opted for a screening that evaluated cytotoxicity in a cell line previously reported to be sensitive to HDAC inhibitors.[8] Briefly, SHSY5Y cells (a patient-derived human neuroblastoma cell line) were treated for 48 h with 10 μM of each compound and viability was evaluated with the MTT assay (Table 1), which measures mitochondrial

* To whom correspondence should be addressed. Tel.: +39-0321-375853 (T.P.); +39-089-962823 (G.B.). Fax: +39-0321-375821 (T.P.); +39-089-969602 (G.B.). E-mail: pirali@pharm.unipmn.it (T.P.); bifulco@nisa.it (G.B.).

[†] Università degli Studi del Piemonte Orientale "A. Avogadro".

[‡] Università di Salerno.

[a] Abbreviations: HDAC, histone deacetylase; SAR, structure−activity relationship; SAHA, suberoylanilide hydroxamic acid; CHAP, cyclic hydroxamic acid-containing peptide; HDLP, histone deacetylase-like protein.

10.1021/jm801529c CCC: $40.75
Published on Web 04/03/2009

Chart 1. From CHAP 1 to the Ugi Products

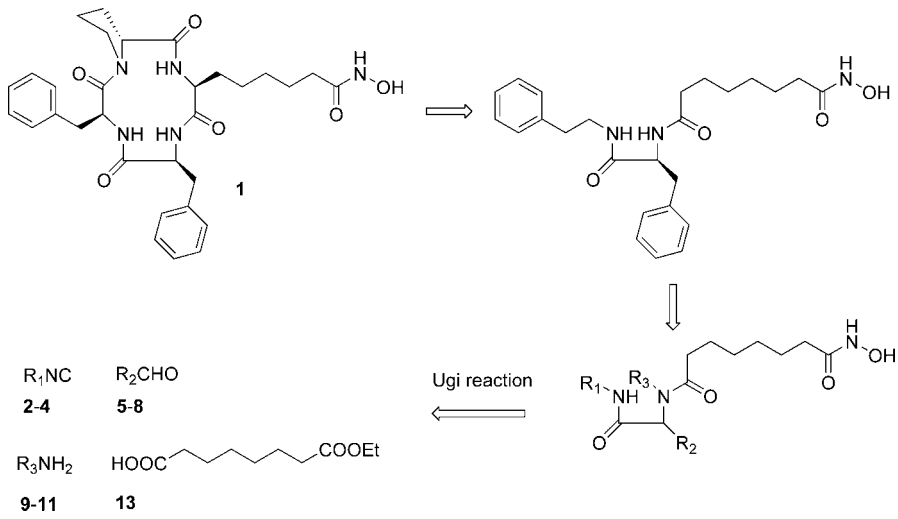

activity. Most compounds possessing the hydroxamates moiety displayed a cytotoxic activity comparable to that of SAHA, chosen as a reference compound. The only exception was represented by **38**, which was unable to induce a significant level of cell death at a concentration of 10 μM. The two benzamide derivatives (**41** and **42**; Table 1), as well as all intermediates tested, were devoid of activity at this concentration (data not shown). To confirm this finding, we performed a full dose−response curve with all the compounds which displayed more than 50% cell death at 10 μM, alongside SAHA. SAHA displayed an IC_{50} of approximately 2.5 $\pm$ 0.1 μM, and **32** (the most potent of the series) displayed an IC_{50} of 2.9 $\pm$ 0.7 μM (Figure 2A). Indeed, all six compounds tested displayed IC_{50}s in the same order of magnitude (range: 2.9−7.5 μM).

To confirm the mechanism of action, we then performed a cellular HDAC activity assay in the same cell line concentrating on SAHA, **32** and **39**. The commercial assay used was the HDAC Fluorimetric Cellular Activity Assay, which measures activity in intact cells. All three compounds inhibited HDAC activity at a concentration of 10 μM, validating the mechanism of action. The rank order of potency (Figure 2B) of the three compounds was SAHA (IC_{50} 0.5 μM $\pm$ 0.1 μM) > **32** (1.2 μM $\pm$ 0.1 μM) > **39** (4.4 μM $\pm$ 0.5 μM). This rank order of potency mirrored the rank order of potency observed in the cytotoxicity assay.

Last, it has been previously reported that a G2/M cell cycle arrest precedes HDAC inhibitors-induced apoptosis in neuroblastoma cells.[8a,9] Indeed, in cells treated for 16 h with 3 μM SAHA the G2/M phase was increased from 12.3 $\pm$ 0.6% to 34 $\pm$ 1% (n = 3). A similar effect was observed with 3 μM **32** (34.3 $\pm$ 2.5%), while no significant effect was

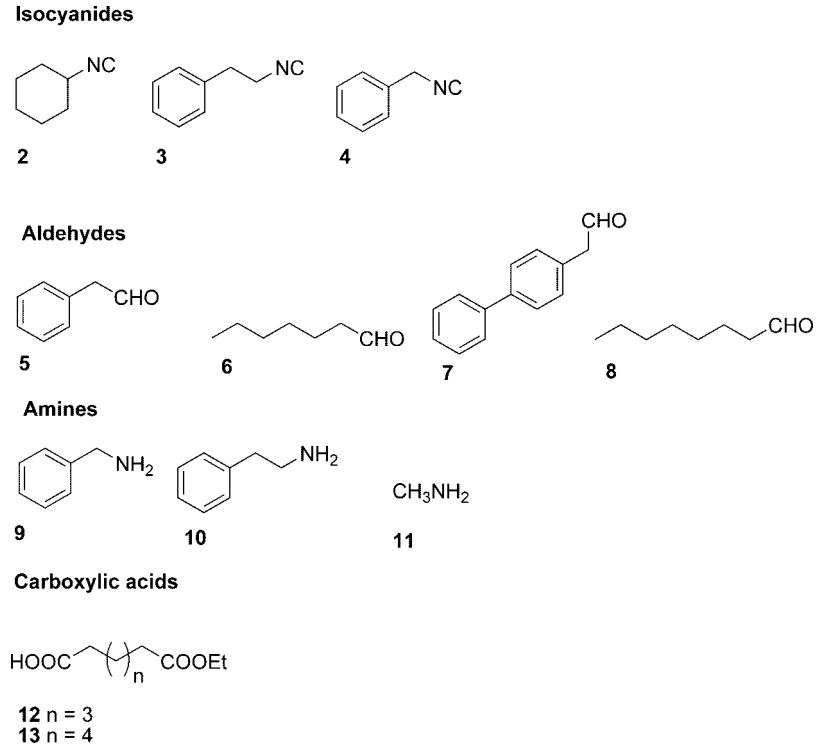

Figure 1. Building blocks.

Scheme 1[a]

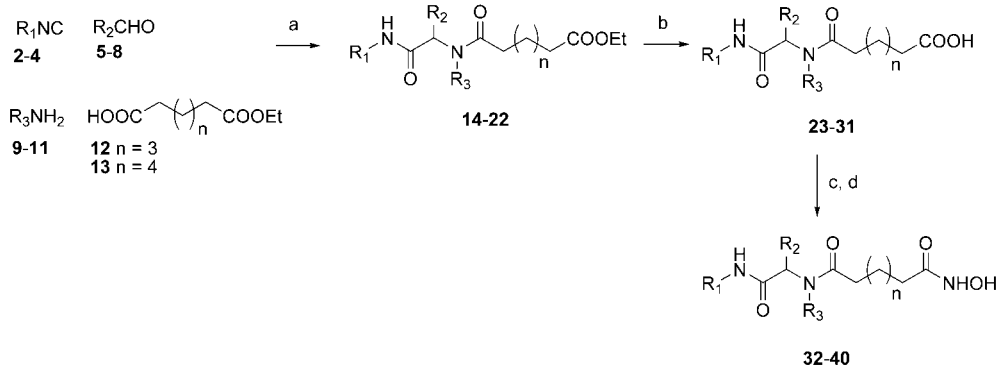

[a] Reagents and conditions: (a) MeOH, rt, 17−44%; (b) LiOH, THF, H_2O, rt, 75−99%; (c) *o*-(*tert*-butyldimethylsilyl)hydroxylamine, TEA, EDCI, CH_2Cl_2, rt; (d) TBAF 1 M in THF, THF, rt, 32−65% (two steps).

Scheme 2[a]

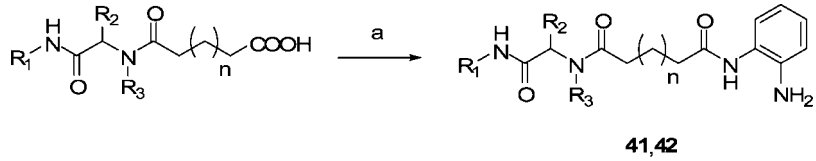

[a] Reagents and conditions: (a) *o*-phenylenediamine, DCC, THF, rt, 23−24%.

Table 1. Synthesized Hydroxamates and Benzamides and their Cytotoxic Activity

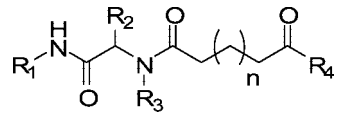

No.	R_1	R_2	R_3	*n*	R_4	viability at 10 μM (% of control)[a]	viability (IC_{50}; μM)	HDAC inhibition (IC_{50}; μM)
32	cyclohexyl	Bn	Bn	3	hydroxamic acid	27.4 ± 0.6	2.5 ± 0.1	1.2 ± 0.1
33	phenethyl	Bn	phenethyl	3	hydroxamic acid	30.2 ± 0.3	2.9 ± 0.7	
34	phenethyl	Bn	Bn	3	hydroxamic acid	30.8 ± 1.8	7.6 ± 4.3	
35	cyclohexyl	hexyl	phenethyl	3	hydroxamic acid	35.0 ± 2.2	2.9 ± 0.3	
36	Bn	Bn	phenethyl	3	hydroxamic acid	34.9 ± 1.4	7.5 ± 3.4	
37	phenethyl	Bn	Bn	4	hydroxamic acid	53.1 ± 1.0		
38	phenethyl	Bn	methyl	4	hydroxamic acid	94.4 ± 2.3		
39	phenethyl	1,1′-diphenyl-4-methylen	Bn	4	hydroxamic acid	22.2 ± 3.1	4.2 ± 0.5	4.4 ± 0.5
40	phenethyl	heptyl	Bn	4	hydroxamic acid	53.0 ± 4.1		
41	cyclohexyl	Bn	Bn	3	benzamide	91.6 ± 2.8		
42	phenethyl	1,1′-diphenyl-4-methylen	Bn	4	benzamide	74.0 ± 4.2		
SAHA						33.8 ± 0.4	2.0 ± 0.2	0.5 ± 0.1

[a] All compounds were screened at a fixed concentration and compounds that exerted significant effects (viability <50% of control) were then characterized with a full concentration response curve. Data are expressed as mean ± SEM of at least six determinations in two experimental days.

observed with the least potent compound (**39**; 3 μM) at this time-point (% of cells in G2/M phase: 11.3 ± 1.5%) (Figure 3).

Discussion and Molecular Docking

To rationalize and to identify the structural features of the active molecules, we performed molecular docking studies on **32** and **39**, both active and structurally dissimilar, and on **38**, which does not display cytotoxic activity, with the HDLP[4] binding pocket (PDB code 1C3R). For docking calculations we used AutoDock 3.0.5 software,[10] which has been successfully used in the interpretation of the inhibitory activity of several HDAC ligands.[11] HDLP (histone deacetylase-like protein) is a zinc−metalloprotein, and this implies a difficulty in finding the appropriate force field parameters for metal centers; in this regard, we considered a nonbonded model for the catalytic center according to the Stote[12] Zn parameters (see Experimental Section). Subsequently, the HDLP active site was refined at QM level, with the aim to obtain a better accordance between theoretical K_i and biological assays results. In particular, the partial charges of the zinc ion and of the amino acids involved in the catalytic center (A169, H170, D168, D258), and the partial charges for the three ligands (**32**, **38**, and **39**) have been calculated at DFT B3LYP level, and the Chelpg[13] method for population analysis (see Experimental Section for details). The efficacy of such QM integration in the docking procedure has provided very promising results in previous studies on the HDAC inhibitors.[11a,d,e]

According to the enzyme mapping, besides the binding channel of 11 Å, there are four hydrophobic cavities (A−D)[11a] acting as molecular recognition domain (Figure 4).

The compounds were obtained in a racemic form; yet, this is one of the limits of the Ugi reaction. Docking studies were performed on both possible configurations (*R* and *S*) for

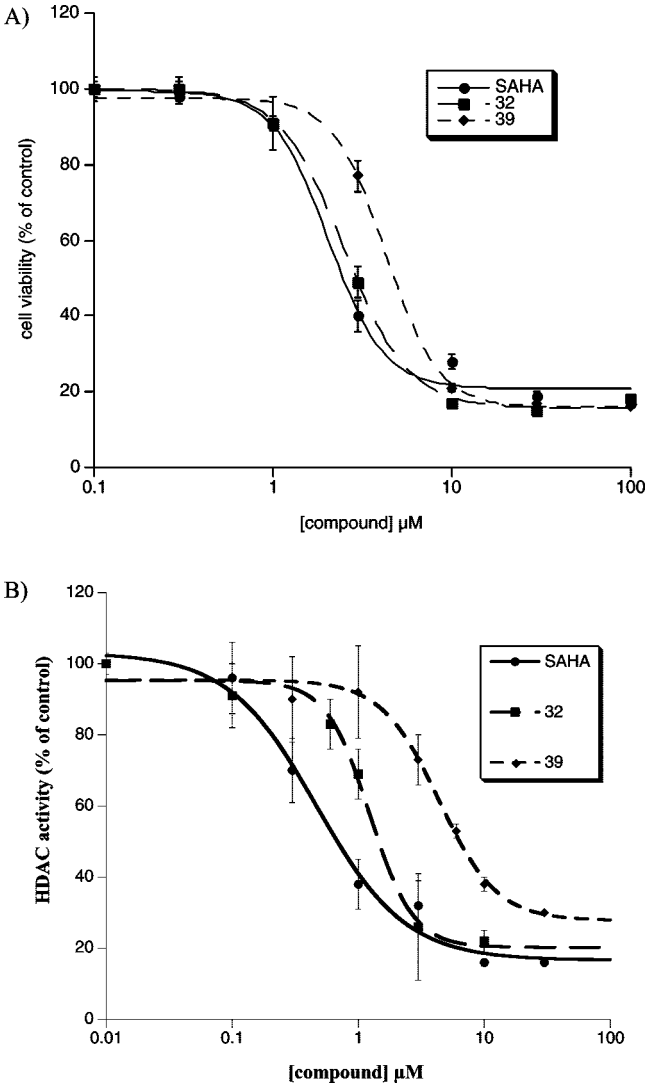

Figure 2. Concentration response curves of SAHA and two selected compounds (**32** and **39**) on cytotoxicity (A) and HDAC inhibition (B). (A) Cytotoxicity was evaluated via the MTT assay and data represent mean ± SEM of 12 replicates in three experimental days. See Table 1 for IC_{50} values. (B) HDAC inhibition was assayed via the Biomol Fluorimetric Cellular Activity Assay in intact cells. Values represent mean ± SEM of 5−9 replicates in two experimental days. See Table 1 for IC_{50} values.

compounds **32**, **38**, and **39**, to evaluate if one or both enantiomers could be actually interacting with the biological target.

In the three-dimensional model (Figure 5a) of the *S*-**32**, it is important to note that the hydroxamic moiety (*metal binder*) is of primary importance for its interactions network: it coordinates the zinc ion in a tridentate fashion and establishes hydrogen bonds with $H^{\varepsilon 2}$ of H132 and OH of Y297 (not shown). The heptanediamide chain (*linker*) makes stabilizing hydrophobic contacts with the zinc-containing tubular pocket. The *cap group*, formed by three rings, establishes noncovalent interactions with the hydrophobic cavities C and D on the HDLP surface (Figure 5a). In particular, the cyclohexylamino ring is correctly accommodated in the D hydrophobic pockets (L265, S266, K267, H170, A197, F198, and F200). The N^1-[1-(phenylmethyl)ethyl] is accommodated in a shallow groove, establishing van der Waals interactions with the macromolecular counterpart, formed by A197 and F200 residues, while the N^1-(phenylmethyl) ring accommodates in the C hydrophobic pockets (P22, F141, H21) of the enzyme.

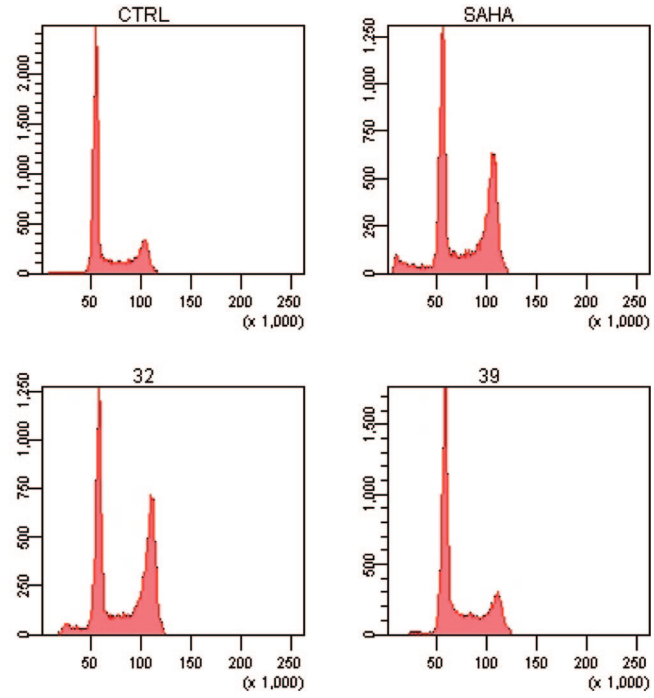

Figure 3. SAHA and **32** induce cell cycle arrest in G2/M phase. Cell cycle analysis of neuroblastoma cells treated for 16 h with the indicated compounds (3 μM). Data are representative of three separate experiments. The *Y*-axis represents cell number and the *X*-axis represents propidium iodide fluorescence on a linear scale.

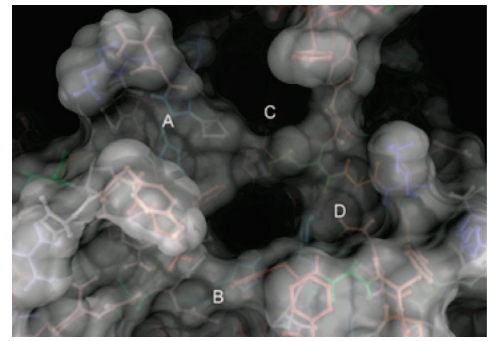

Figure 4. 3D model of the HDLP. The protein is represented by molecular surface and sticks and balls.

Figure 5b depicts the 3D model of the interaction between *R*-**32** and the target; the *metal binder*, *linker chain*, and the *cap group* of the two docked enantiomers (*R*- and *S*-**32**) fill equivalent spaces, but the two rings (cyclohexylamino and N^1-[1-(phenylmethyl)ethyl]) of the *cap group* are in inverted positions on the HDLP surface with respect to *S*-**32** (Figure 5b). In particular, the cyclohexylamino ring interacts with the A197, and F200 residues, while the N^1-[1-(phenylmethyl)ethyl] is accommodated in D pocket (L265, S266, K267, H170, A197, F198, and F200); in the mean time, the N^1-(phenylmethyl) remains interacting with the aminoacid of the C hydrophobic pocket (P22, F141, H21). The different arrangement of the *R*-**32** and the suboptimal hydrophobic interactions are responsible for a predicted decrease in the binding affinity to the receptor of about 2.5-fold (K_i of *S*-**32** 4.45×10^{-8} vs K_i of the enantiomer 1.04×10^{-7}).

The same approach was used for **39**. Keeping in mind the 3D model of the interactions between **32** and the HDLP binding site described above, the octanediamide chain of *S*-**39** fits into the 11 Å channel (Figure 6a), the NHOH group binds to the

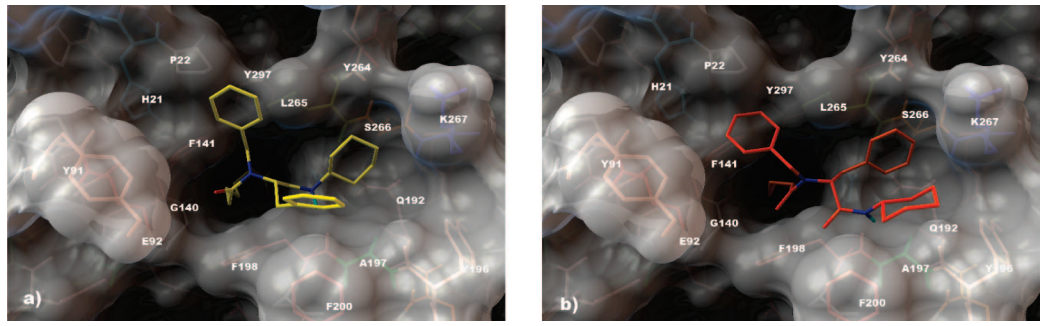

Figure 5. (a) 3D model of the interaction between *S*-**32** and the HDLP binding site. The protein is represented by molecular surface and sticks and balls. *S*-**32** is depicted by sticks (by atom type: C, yellow; polar H, sky-blue; N, dark blue; O, red). (b) 3D model of the interaction between *R*-**32** and the HDLP binding site. The protein is represented by molecular surface and sticks and balls. *R*-**32** is depicted by sticks (by atom type: C, orange; polar H, sky-blue; N, dark-blue; O, red).

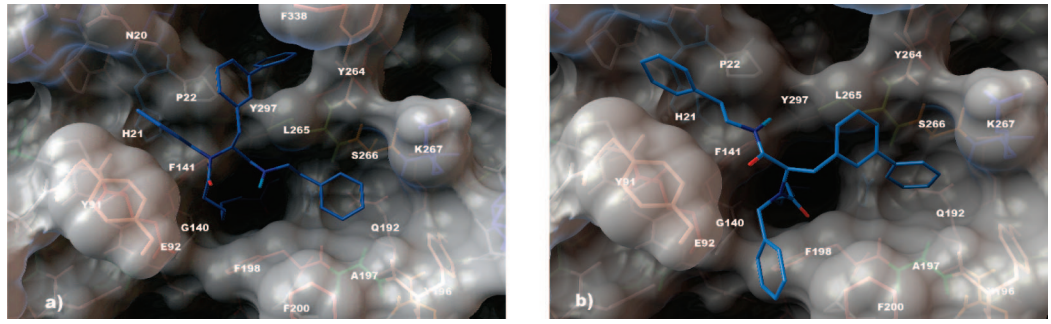

Figure 6. (a) 3D model of the interaction between *S*-**39** and the HDLP binding site. The protein is represented by molecular surface and sticks and balls. *S*-**39** is depicted by sticks (by atom type: C, blue; polar H, sky-blue; N, dark blue; O, red). (b) 3D model of the interaction between *R*-**39** and the HDLP binding site. The protein is represented by molecular surface and sticks and balls. *R*-**39** is depicted by sticks (by atom type: C, light-blue; polar H, sky-blue; N, dark blue; O, red).

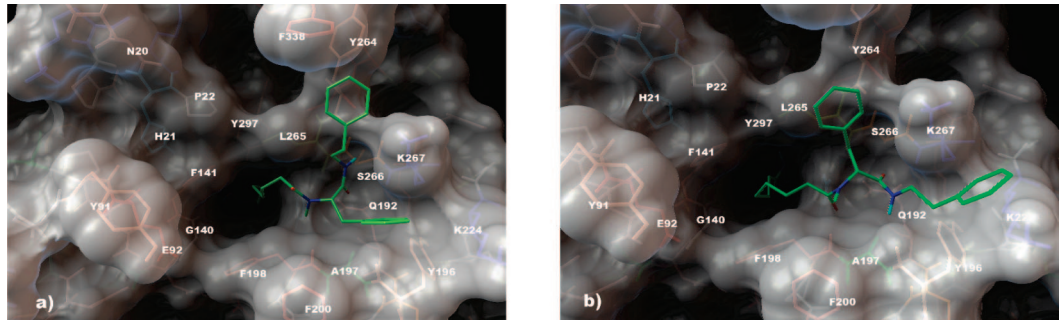

Figure 7. (a) 3D model of the interaction between *S*-**38** and the HDLP binding site. The protein is represented by molecular surface and sticks and balls. *S*-**38** is depicted by sticks (by atom type: C, light-green; polar H, sky-blue; N, dark blue; O, red). (b) 3D model of the interaction between *R*-**38** and the HDLP binding site. The protein is represented by molecular surface and sticks and balls. *R*-**38** is depicted by sticks (by atom type: C, green; polar H, sky-blue; N, dark blue; O, red).

Zn^{2+} ion, at the bottom of the channel, in a tridentate fashion and establishes hydrogen bonds with $H^{\varepsilon 2}$ of H132, $O^{\varepsilon 2}$ of D258, and OH of Y297 (not shown). The *cap group*, formed by four aromatic rings, establishes hydrophobic interactions with the cavities (A, C, and D). The N^1-[1-([1,1′-biphenyl]-methyl)]ethyl] group accommodates in pocket C (P22, F141, Y264, Y297). The N^1-[(2-phenylethyl)amino]ethyl] ring accommodates in pocket D (L265, S266, K267, H170, A197, F198, and F200), while the N^1-(phenylmethyl) occupies pocket A (P22, Y91, E92, and F141).

Figure 6b depicts the putative three-dimensional model of *R*-**39**−HDLP complex. Comparing this model with the *S*-enantiomer binding mode, the only difference is the R_1−R_3 arrangement on the enzyme surface; in particular, the pockets A and D are occupied by the N^1-(phenylmethyl) and the N^1-[1-([1,1′-biphenyl]-methyl)]ethyl] moieties, respectively, while the N^1-[(2-phenylethyl)amino]ethyl] ring interacts with the F198, F200, and Y91 amino acids. The minor efficiency of such interactions are responsible of a small decrease in the binding affinity to the target (of about 5-fold: K_i of *S*-**39** 7.69×10^{-9} vs K_i of the enantiomer 3.86×10^{-8}).

In both the enantiomers *R* and *S* of **38**, the lack of a hydrophobic and bulky group on R_3 is responsible for a predicted decreased histone deacetylase inhibitory activity (K_i of *S*-**38** 2.44×10^{-7} vs K_i of the enantiomer 3.87×10^{-7}), because their expected noncovalent interactions are lost. In the first model (Figure 7a), the N^8-[2-[(2-phenylethyl)amino], and N^8-1-(phenylmethyl)ethyl groups are placed in D (L265, S266, K267, H170, A197, F198, and F200) hydrophobic cavity, but the hydroxamic moiety (*metal binder*) coordinates the zinc ion in a monodentate fashion. In the three-dimensional model of *R*-**38**, the R_1 and R_2 substituents are placed in the same hydrophobic cavity found for the *S*-enantiomer but with an inverted spatial

arrangement, while the NHOH group binds to the Zn ion in a bidentate fashion.

Keeping in mind the biological results and the descriptions of the 3D models of **32**, **38**, and **39** with HDLP discussed above, we offer here a rationalization of our results related to compounds containing $NHR_1COCHR_2NR_3$ as *cap group*. In particular, the influence of the hydrophobic and bulky group on R_1, R_2, and R_3, in turn related especially to hydrophobic interactions, and to aromatic stacking, seem to be the driving forces of the target−ligand complexes. Such evidence is confirmed by calculated and experimental **38** inactivity.

In light of the above results and thanks to the good qualitative accordance between the results of biological essays and the prediction of the molecular docking calculations, there is a complete rationalization of the putative binding mode for **32**, **38**, and **39** enantiomers pairs. In particular, a new scaffold was proven to be an efficient *cap group* model in the rational design of new linear HDAC inhibitors, and the critical features necessary for the optimal contact modes with HDLP binding pocket were determined.

Experimental Section

Chemistry. Commercially available reagents and solvents were used without further purification and were purchased from Fluka-Aldrich or Lancaster. Aldehydes (phenylacetaldehyde, heptanal, octanal) were distilled under vacuum immediately before use. Dichloromethane was dried by distillation from P_2O_5 and stored on activated molecular sieves (4 Å). Dimethylsulfoxide was dried by distillation under vacuum and stored on activated molecular sieves (4 Å). Tetrahydrofuran and diethyl ether were distilled immediately before use from Na/benzophenone under a slight positive atmosphere of nitrogen. When needed, the reactions were performed in oven-dried glassware under a positive pressure of dry nitrogen.

Melting points were determined in open glass capillary with a Stuart scientific SMP3 apparatus and are uncorrected. All the compounds were checked by IR (FT-IR THERMO-NICOLET AVATAR), ^{1}H and ^{13}C APT (JEOL ECP 300 MHz), and mass spectrometry (Thermo Finningan LCQ-deca XP-*plus*) equipped with an ESI source and an ion trap detector. Chemical shifts are reported in part per million (ppm). Column chromatography was performed on silica gel (Merck Kieselgel 70−230 mesh ASTM) using the indicated eluants. Thin layer chromatography (TLC) was carried out on 5 × 20 cm plates with a layer thickness of 0.25 mm (Merck Silica gel 60 F_{254}). When necessary they were developed with $KMnO_4$ or iron trichloride. Purity of tested compounds was estabilished by elemental analysis. Elemental analysis (C, H, N) of the target compounds are within ±0.4% of the calculated values, confirming ≥95% purity.

2-Phenylethylisocyanide (3). 2-Phenylethylamine (8.51 g, 70.4 mmol, 1 equiv) and methyl formate (10.8 mL, 176.0 mmol, 2.5 equiv) were heated at reflux for 12 h. Removal of excess methyl formate under reduced pressure gave the formamide derivative, which is used in the next step without further purification.

2-Phenylethylformamide is dissolved in dichloromethane (100 mL). To the cooled (−10 °C) solution, TEA (49.0 mL, 351.8 mmol, 5 equiv) is added and a solution of $POCl_3$ (10.0 mL, 105.5 mmol, 1.5 equiv) in dichloromethane (50 mL) is added dropwise under nitrogen atmosphere. The resulting suspension is stirred for 3 h at −10 °C and quenched by addition of sat. aq. $NaHCO_3$. The organic layer is separated, washed with sat. aq. $NaHCO_3$ (×2) and brine (×1), dried over sodium sulfate, and evaporated. The crude material is purified by column chromatography, using petroleum ether/EtOAc 5:5 as eluant to give the isocyanide as a yellow oil (8.30 g; 77%). ^{1}H NMR (300 MHz, $CDCl_3$) δ 7.35−7.22 (m, 5-H), 3.59 (t, J = 1.9 Hz, 2-H), 2.97 (t, J = 1.9 Hz, 2-H); ^{13}C NMR (75 MHz, $CDCl_3$) δ 156.7, 136.8, 128.9, 128.8, 127.4, 43.0, 35.7; MS (ESI) m/z 132 $(M + H)^+$.

4-Biphenylacetaldehyde (7). 4-Biphenylacetic acid (4.60 g, 21.7 mmol, 1 equiv) is dissolved in methanol (70 mL), and thionyl chloride (3.00 mL, 43.3 mmol, 2 equiv) is added at 0 °C. The solution is heated at reflux. After 2 h, the reaction is evaporated, diluted with EtOAc, and washed with $NaHCO_3$ (×2) and brine (×1) and dried over sodium sulfate. The solvent is evaporated to give the methyl ester, which is used in the next step without further purification.

4-Biphenylmethylacetate is dissolved in diethyl ether (50 mL) and added to a suspension of $LiAlH_4$ (823 mg, 21.7 mmol, 1 equiv) in diethyl ether (50 mL) at 0 °C. The reaction is quenched by addition of sat. aq. sodium sulfate dropwise under stirring and a white precipitate is formed. The suspension is filtered through a pad of Celite and the filtrate is washed with brine (×1), dried over sodium sulfate, and evaporated to give the alcohol, which is used in the next step without further purification.

4-Biphenylethanol is dissolved in DMSO (200 mL) and IBX (2-iodoxybenzoic acid) (13.8 g, 32.5 mmol, 1.5 equiv) is added portionwise. After 3 h, water and diethyl ether are added. The resulting suspension is filtered under vacuum. The aqueous layer is extracted with diethyl ether (×4), and the combined organic phases are washed with water (×3) and brine (×1), dried over sodium sulfate, and evaporated to give the aldehyde as an orange oil (3.82 g; 90%). ^{1}H NMR (300 MHz, $CDCl_3$) δ 9.79 (t, J = 2.5 Hz, 1-H), 7.61−7.31 (m, 9-H), 3.74 (d, J = 2.5 Hz, 1-H); ^{13}C NMR (75 MHz, $CDCl_3$) δ 199.4, 140.7, 140.5, 130.9, 130.1, 128.9, 127.8, 127.5, 127.2; MS (ESI) m/z 197 $(M + H)^+$.

General Procedure for the Preparation of Carboxylic Acids (12, 13). The corresponding diethyl ester (diethyl pimelate, diethyl suberate; 1 equiv) is dissolved in ethanol and a solution of KOH (1 equiv) in ethanol is added dropwise. The reaction is heated to 50 °C for 12 h. The ethanol is evaporated and the white solid is dissolved with 2 N HCl and extracted with dichloromethane (×2). The combined organic layers are washed with brine, dried over sodium sulfate, and evaporated. The crude material is purified by column cromatography, using petroleum ether/EtOAc 5:5 as eluant to give the carboxylic acid.

7-Ethoxy-7-oxoheptanoic acid (12). Colorless oil (55%); ^{1}H NMR (300 MHz, $CDCl_3$) δ 4.10 (q, J = 7.1 Hz, 2-H), 2.30 (quint, J = 7.4 Hz, 4-H), 1.63 (m, 4-H), 1.35 (m, 2-H), 1.23 (t, J = 7.1 Hz, 3-H).

8-Ethoxy-8-oxooctanoic acid (13). Colorless oil (49%); ^{1}H NMR (300 MHz, $CDCl_3$) δ 4.10 (q, J = 7.1 Hz, 2-H), 2.30 (quint, J = 7.4 Hz, 4-H), 1.62 (m, 4-H), 1.33 (m, 4-H), 1.24 (t, J = 7.1 Hz, 3-H).

General Procedure for the Ugi Reaction (14−22). The aldehyde (1.2 equiv) is dissolved in methanol (2 M), and the amine (1.2 equiv) is added. After 15 min, the carboxylic acid (1 equiv) and the isocyanide (1 equiv) are added under a nitrogen atmosphere. The reaction is stirred at room temperature for 48 h. The solvent is evaporated and the crude material is purified by column cromatography to give the Ugi product.

Heptanoic Acid, 7-[[2-(Cyclohexylamino)-2-oxo-1-(phenylmethyl)ethyl](phenylmethyl)amino]-7-oxo-, Ethyl Ester (14). The crude material is purified by column chromatography, using petroleum ether/EtOAc 7:3 as eluant to give a light yellow solid (44%). IR (KBr) 3287, 2359, 2342, 1730, 1624, 1254, 1129, 1030, 748, 668 cm^{-1}; ^{1}H NMR (300 MHz, $CDCl_3$) δ 7.28−7.16 (m, 10-H), 6.24 (d, J = 7.9 Hz, 1-H), 5.03 (t, J = 8.0 Hz, 1-H), 4.62 (d, J = 17.6 Hz, 1-H), 4.46 (d, J = 17.6 Hz, 1-H), 4.09 (q, J = 7.1 Hz, 2-H), 3.59 (m, 1-H), 3.20 (m, 1-H), 3.00 (m, 1-H), 2.22 (m, 4-H), 1.82−1.51 (m, 10-H), 1.35−1.19 (m, 9-H); ^{13}C NMR (75 MHz, $CDCl_3$) δ 175.2, 173.5, 169.2, 137.6, 137.5, 130.2, 129.2, 128.8, 128.5, 127.4, 126.3, 60.5, 60.1, 49.6, 48.0, 35.0, 34.1, 33.8, 32.7, 28.8, 25.6, 25.0, 24.7, 24.6, 14.3; MS (ESI) m/z 529 $(M + Na)^+$; Mp = 71−73 °C.

Heptanoic Acid, 7-Oxo-7-[[2-oxo-2-[(2-phenylethyl)amino]-1-(phenylmethyl)ethyl](2-phenylethyl)amino]-, Ethyl Ester (15). The crude material is purified by column chromatography, using petroleum ether/EtOAc 8:2 as eluant to give a yellow oil (26%). IR (KBr) 2359, 2341, 1731, 1626, 1453, 1260, 1178, 1029, 668

cm^{-1}; ^{1}H NMR (300 MHz, $CDCl_3$) δ 7.37−7.16 (m, 15-H), 6.72 (br t, 1-H), 4.88 (t, J = 7.1 Hz, 1-H), 4.10 (q, J = 7.1 Hz, 2-H), 3.55−3.15 (m, 6-H), 2.88−2.45 (m, 4-H), 2.27 (t, J = 7.4 Hz, 2-H), 2.10 (m, 2-H), 1.61−1.40 (m, 4-H), 1.24 (m, 5-H); ^{13}C NMR (75 MHz, $CDCl_3$) δ 174.6, 173.7, 171.0, 138.9, 138.1, 137.5, 129.1, 129.0, 128.8, 128.6, 128.7, 128.5, 127.0, 126.8, 126.5, 60.3, 54.2, 48.5, 40.6, 35.8, 35.6, 34.5, 34.2, 33.4, 28.8, 24.9, 24.8, 14.3; MS (ESI) m/z 565 (M + Na)$^+$.

Heptanoic Acid, 7-Oxo-7-[[2-oxo-2-[(2-phenylethyl)amino]-1-(phenylmethyl)ethyl](phenylmethyl)amino]-, Ethyl Ester (16). The crude material is purified by column chromatography, using petroleum ether/EtOAc 7:3 as eluant to give a yellow oil (18%). IR (KBr) 2936, 1728, 1627, 1453, 1199, 1029, 731, 647 cm^{-1}; ^{1}H NMR (300 MHz, $CDCl_3$) δ 7.35−7.02 (m, 15-H), 6.53 (t, J = 5.5 Hz, 1-H), 5.04 (t, J = 7.7 Hz, 1-H), 4.53 (d, J = 17.6 Hz, 1-H), 4.41 (d, J = 17.6 Hz, 1-H), 4.08 (q, J = 7.1 Hz, 2-H), 3.47−3.19 (m, 3-H), 2.99 (m, 1-H), 2.64 (m, 2-H), 2.21 (t, J = 7.4 Hz, 2-H), 2.16 (t, J = 7.4 Hz, 2-H), 1.61−1.45 (m, 4-H), 1.24−1.19 (m, 5-H); ^{13}C NMR (75 MHz, $CDCl_3$) δ 175.1, 173.7, 170.1, 138.9, 137.5, 137.4, 129.4, 129.1, 128.9, 128.6, 128.5, 128.4, 127.0, 126.8, 126.5, 60.3, 59.9, 49.3, 40.5, 35.5, 35.3, 34.1, 33.7, 28.7, 24.8, 24.7, 14.5; MS (ESI) m/z 551 (M + Na)$^+$.

Heptanoic Acid, 7-[[1-[(Cyclohexylamino)carbonyl]heptyl](2-phenylethyl)amino]-7-oxo-, Ethyl Ester (17). The crude material is purified by column chromatography, using petroleum ether/EtOAc 8:2 as eluant to give a light yellow oil (22%). IR (KBr) 2929, 2855, 1734, 1625, 1534, 1452, 1255, 1179, 1030 cm^{-1}; ^{1}H NMR (300 MHz, $CDCl_3$) δ 7.31−7.10 (m, 5-H), 6.54 (d, J = 8.2 Hz, 1-H), 4.75 (t, J = 7.7 Hz, 1-H), 4.10 (q, J = 7.1 Hz, 2-H), 3.72 (m, 1-H), 3.45 (m, 2-H), 2.87 (m, 1-H), 2.74 (m, 1-H), 2.29 (m, 4-H), 2.03−1.54 (m, 12-H), 1.43−1.18 (m, 14-H), 0.85 (m, 6-H); ^{13}C NMR (75 MHz, $CDCl_3$) δ 174.6, 173.7, 170.5, 138.3, 128.8 (2C), 126.8, 60.3, 58.0, 47.9, 47.1, 36.4, 34.2, 33.4, 32.9, 31.7, 29.2, 29.0, 28.2, 26.2, 25.6, 25.2, 24.8, 24.7, 22.6, 14.3, 14.1; MS (ESI) m/z 537 (M + Na)$^+$.

Heptanoic Acid, 7-Oxo-7-[[2-oxo-1-(phenylmethyl)-2-[(phenylmethyl)amino]ethyl](2-phenylethyl)amino]-, Ethyl Ester (18). The crude material is purified by column chromatography, using petroleum ether/EtOAc 7:3 as eluant to give a yellow oil (17%). IR (KBr) 1731, 1625, 1529, 1453, 1259, 1178, 1029, 748 cm^{-1}; ^{1}H NMR (300 MHz, $CDCl_3$) δ 7.36−7.04 (m, 15-H), 5.03 (t, J = 7.7 Hz, 1-H), 4.43 (d, J = 5.8 Hz, 2-H), 4.09 (q, J = 7.1 Hz, 2-H), 3.50−3.22 (m, 4-H), 2.68 (m, 2-H), 2.23 (t, J = 7.4 Hz, 2-H), 2.13 (m, 2-H), 1.53 (m, 4-H), 1.21 (m, 5-H); ^{13}C NMR (75 MHz, $CDCl_3$) δ 174.7, 173.6, 170.8, 138.2 (2C), 137.4, 129.3, 128.8, 128.7, 128.6 (2C), 127.7, 127.4, 126.8, 126.7, 60.5, 60.3, 48.4, 43.4, 36.0, 34.6, 34.1, 33.4, 28.8, 24.9, 24.7, 14.4; MS (ESI) m/z 551 (M + Na)$^+$.

Octanoic Acid, 8-[[(2-Methylphenyl)methyl][2-oxo-2-[(2-phenylethyl)amino]-1-(phenylmethyl)ethyl]amino]-8-oxo-, Ethyl Ester (19). The crude material is purified by column chromatography, using petroleum ether/EtOAc 7:3 as eluant to give a yellow oil (19%). IR (KBr) 1731, 1629, 1453, 1179, 1030, 730, 697 cm^{-1}; ^{1}H NMR (300 MHz, $CDCl_3$) δ 7.28−6.99 (m, 15-H), 6.71 (t, J = 5.5 Hz, 1-H), 5.06 (t, J = 7.4 Hz, 1-H), 4.51 (d, J = 17.6 Hz, 1-H), 4.35 (d, J = 17.6 Hz, 1-H), 4.01 (q, J = 7.1 Hz, 2-H), 3.39−3.12 (m, 3-H), 2.93 (m, 1-H), 2.56 (m, 2-H), 2.16 (t, J = 7.1 Hz, 2-H), 2.09 (m, 2-H), 1.53 (m, 4-H), 1.48 (m, 4-H), 1.15 (m, 7-H); ^{13}C NMR (75 MHz, $CDCl_3$) δ 175.0, 173.6, 170.0, 139.0, 137.6 (2C), 129.3, 128.7, 128.6, 128.5, 128.4, 127.3, 126.6, 126.3, 126.2, 60.1, 59.7, 49.1, 40.5, 35.5, 35.0, 34.2, 33.7, 28.8 (2C), 25.0, 24.8, 14.3; MS (ESI) m/z 565 (M + Na)$^+$.

Octanoic Acid, 8-[Methyl[2-oxo-2-[(2-phenylethyl)amino]-1-(phenylmethyl)ethyl]amino]-8-oxo-, Ethyl Ester (20). The crude material is purified by column chromatography, using petroleum ether/EtOAc 7:3 as eluant to give a colorless oil (18%). IR (KBr) 2933, 2361, 1731, 1630, 1454, 1259, 1177, 1030, 699 cm^{-1}; ^{1}H NMR (300 MHz, $CDCl_3$) δ 7.29−6.89 (m, 10-H), 6.19 (br t, 1-H), 5.28 (t, J = 7.1 Hz, 1-H), 4.09 (q, J = 7.1 Hz, 2-H), 3.44 (m, 2-H), 3.23 (m, 1-H), 2.75 (s, 3-H), 2.69 (m, 2-H), 2.23 (t, J = 7.4 Hz, 2-H), 2.09 (m, 2-H), 1.54 (m, 2-H), 1.41 (m, 2-H), 1.19 (m, 7-H); ^{13}C NMR (75 MHz, $CDCl_3$) δ 174.0, 173.5, 170.1, 138.8, 137.3, 128.9, 128.7, 128.6, 126.8, 126.6, 126.5, 60.2, 56.9, 40.3, 35.4, 34.1, 34.0, 33.4, 30.9, 28.8, 28.7, 24.7, 24.6, 14.2; MS (ESI) m/z 489 (M + Na)$^+$.

Octanoic Acid, 8-[[1-([1,1′-Biphenyl]-4-ylmethyl)-2-oxo-2-[(2-phenylethyl)amino]ethyl](phenylmethyl)amino]-8-oxo-, Ethyl Ester (21). The crude material is purified by column chromatography, using petroleum ether/EtOAc 8:2 as eluant to give a white solid (43%). IR (KBr) 3266, 2943, 1731, 1674, 1618, 1192, 833, 768, 730 cm^{-1}; ^{1}H NMR (300 MHz, $CDCl_3$) δ 7.55−7.05 (m, 19-H), 6.53 (br t, 1-H), 5.08 (br t, 1-H), 4.51 (m, 2-H), 4.09 (q, J = 7.1 Hz, 2-H), 3.42−3.21 (m, 3-H), 3.04 (m, 1-H), 2.68 (m, 2-H), 2.23 (m, 4-H), 1.55 (m, 4-H), 1.23 (m, 7-H); ^{13}C NMR (75 MHz, $CDCl_3$) δ 175.3, 173.7, 170.1, 140.8, 139.5, 138.9, 137.4, 136.6, 129.8, 128.9 (2C), 128.8, 128.5, 127.4, 127.3, 127.1, 127.0, 126.5, 126.3, 60.2, 59.9, 49.3, 40.5, 35.5, 34.5, 34.2, 33.8, 28.9 (2C), 25.0, 24.8, 14.4; MS (ESI) m/z 641 (M + Na)$^+$; Mp = 77−79 °C.

Octanoic Acid, 8-Oxo-8-[[1-[[(2-phenylethyl)amino]carbonyl]-octyl](phenylmethyl)amino]-, Ethyl Ester (22). The crude material is purified by column chromatography, using petroleum ether/EtOAc 7:3 as eluant to give a colorless oil (24%). IR (KBr) 2927, 2360, 1733, 1628, 1453, 1178, 1030, 749, 698 cm^{-1}; ^{1}H NMR (300 MHz, $CDCl_3$) δ 7.55−7.02 (m, 10-H), 6.78 (t, J = 5.5 Hz, 1-H), 4.82 (t, J = 6.3 Hz, 1-H), 4.45 (m, 2-H), 3.97 (q, J = 7.1 Hz, 2-H), 3.33 (m, 2-H), 2.67 (t, J = 7.1 Hz, 2-H), 2.10 (m, 4-H), 1.77 (m, 1-H), 1.44 (m, 5-H), 1.09 (m, 17-H), 0.75 (t, J = 6.9 Hz, 3-H); ^{13}C NMR (75 MHz, $CDCl_3$) δ 175.4, 173.8, 170.9, 138.9, 137.8, 128.8, 128.7, 128.6, 127.3, 126.5, 126.0, 60.3, 57.9, 48.4, 40.3, 35.7, 34.3, 33.7, 31.8, 29.4, 29.1, 28.9 (2C), 28.3, 26.5, 25.1, 24.8, 22.6, 14.3, 14.2; MS (ESI) m/z 573 (M + Na)$^+$.

General Procedure for the Saponification Reaction (23−31). The ethyl ester (1 equiv) is dissolved in THF and water (2:1) and LiOH (3 equiv) is added. The reaction is stirred at room temperature for 12 h. The volatile is evaporated and the crude material is purified by column cromatography to give the carboxylic acid.

7-[[2-(Cyclohexylamino)-2-oxo-1-(phenylmethyl)ethyl](phenylmethyl)amino]-7-oxo-heptanoic Acid (23). The crude material is purified by column chromatography, using petroleum ether/EtOAc 6:4 (+ formic acid 1%) as eluant to give a colorless oil (81%). IR (KBr) 3260, 2931, 2360, 1721, 1608, 1288, 1190, 976, 733, 587 cm^{-1}; ^{1}H NMR (300 MHz, $CDCl_3$) δ 10.39 (br s, 1-H), 7.28−7.01 (m, 10-H), 6.47 (d, J = 8.0 Hz, 1-H), 5.07 (t, J = 8.0 Hz, 1-H), 4.64 (d, J = 17.6 Hz, 1-H), 4.48 (d, J = 17.6 Hz, 1-H), 3.59 (m, 1-H), 3.18 (m, 1-H), 3.00 (m, 1-H), 2.22 (m, 4-H), 1.88−1.47 (m, 10-H), 1.34−1.05 (m, 6-H); ^{13}C NMR (75 MHz, $CDCl_3$) δ 178.1, 175.6, 169.2, 137.4 (2C), 129.3, 128.8, 128.5, 127.4, 126.7, 126.2, 60.2, 49.4, 48.1, 35.0 (2C), 32.6, 28.7, 25.3, 24.9, 24.6, 24.5 (2C); MS (ESI) m/z 501 (M + Na)$^+$.

7-Oxo-7-[[2-oxo-2-[(2-phenylethyl)amino]-1-(phenylmethyl)ethyl](2-phenylethyl)amino]-heptanoic Acid (24). The crude material is purified by column chromatography, using petroleum ether/EtOAc 5:5 (+ formic acid 1%) as eluant to give a light yellow oil (92%). IR (KBr) 2936, 1719, 1639, 1602, 1454, 1178, 1029, 896, 748 cm^{-1}; ^{1}H NMR (300 MHz, $CDCl_3$) δ 8.02 (s, 1-H), 7.38−7.12 (m, 15-H), 4.92 (t, J = 7.4 Hz, 1-H), 3.58−3.16 (m, 6-H), 2.78−2.49 (m, 4-H), 2.32 (t, J = 7.4 Hz, 2-H), 2.10 (m, 2-H), 1.64−1.43 (m, 4-H), 1.25 (m, 2-H); ^{13}C NMR (75 MHz, $CDCl_3$) δ 178.2, 175.3, 171.2, 138.9, 138.0, 137.1, 129.1, 129.0, 128.9, 128.8, 128.6, 128.5, 127.0, 126.8, 126.5, 53.7, 48.9, 40.9, 35.8, 35.3, 34.6, 33.9, 33.4, 28.8, 24.9, 24.6; MS (ESI) m/z 537 (M + Na)$^+$.

7-Oxo-7-[[2-oxo-2-[(2-phenylethyl)amino]-1-(phenylmethyl)ethyl](phenylmethyl)amino]-heptanoic Acid (25). The crude material is purified by column chromatography, using petroleum ether/EtOAc 5:5 (+ formic acid 1%) as eluant to give a light yellow oil (75%). IR (KBr) 1723, 1624, 1453, 1199, 1029, 973, 729 cm^{-1}; ^{1}H NMR (300 MHz, $CDCl_3$) δ 7.36−7.01 (m, 15-H), 6.57 (t, J = 5.5, 1-H), 5.06 (t, J = 7.9 Hz, 1-H), 4.48 (m, 2-H), 3.49−3.15 (m, 3-H), 2.98 (m, 1-H), 2.64 (m, 2-H), 2.26 (t, J = 7.4 Hz, 2-H), 2.15 (t, J = 7.4 Hz, 2-H), 1.53 (m, 4-H), 1.24 (m, 2-H); ^{13}C NMR (75 MHz, $CDCl_3$) δ 175.3, 172.9, 170.1, 138.9, 137.5, 137.4, 129.4, 129.1, 128.9, 128.6, 128.5, 128.0, 127.0, 126.8, 126.5, 60.3, 49.3, 40.6, 35.5, 35.3 (2C), 33.7, 28.7, 24.8, 24.7; MS (ESI) m/z 523 (M + Na)$^+$.

7-[[1-[(Cyclohexylamino)carbonyl]heptyl](2-phenylethyl)amino]-7-oxo-heptanoic Acid (26). The crude material is purified by column chromatography, using petroleum ether/EtOAc 5:5 (+ formic acid 1%) as eluant to give a light yellow oil (82%). IR (KBr) 2928, 2855, 2360, 1718, 1623, 1452, 1259, 1198, 891, 700, 614 cm^{-1}; ^1H NMR (300 MHz, $CDCl_3$) δ 10.63 (br s, 1-H), 7.38−7.05 (m, 5-H), 6.85 (d, J = 8.2 Hz, 1-H), 4.77 (t, J = 7.4 Hz, 1-H), 3.68 (m, 1-H), 3.44 (m, 2-H), 2.81 (m, 1-H), 2.68 (m, 1-H), 2.25 (m, 4-H), 2.05−1.48 (m, 12-H), 1.33−1.07 (m, 14-H), 0.80 (m, 3-H); ^{13}C NMR (75 MHz, $CDCl_3$) δ 177.3, 174.8, 170.5, 138.1, 128.2, 126.7, 125.3, 60.3, 48.0, 47.2, 36.4, 33.9, 33.3, 32.7, 31.6, 29.0, 28.8, 28.5, 26.1, 25.6, 25.1, 24.7 (2C), 22.6, 14.1; MS (ESI) m/z 509 $(M + Na)^+$.

7-Oxo-7-[[2-oxo-1-(phenylmethyl)-2-[(phenylmethyl)amino]ethyl](2-phenylethyl)amino]-heptanoic Acid (27). The crude material is purified by column chromatography, using petroleum ether/EtOAc 4:6 (+ formic acid 1%) as eluant to give a yellow oil (68%). IR (KBr) 1719, 1623, 1496, 1453, 1259, 1178, 748 cm^{-1}; ^1H NMR (300 MHz, $CDCl_3$) δ 7.43 (br t, 1-H), 7.33−7.09 (m, 15-H), 5.11 (t, J = 7.7 Hz, 1-H), 4.42 (m, 2-H), 3.54−3.23 (m, 4-H), 2.68 (m, 2-H), 2.29 (t, J = 7.4 Hz, 2-H), 2.16 (m, 2-H), 1.51 (m, 4-H), 1.21 (m, 2-H); ^{13}C NMR (75 MHz, $CDCl_3$) δ 178.4, 175.1, 170.8, 138.3, 138.1, 137.2, 129.3, 128.8, 128.7, 128.6 (2C), 127.7, 127.4, 126.8, 126.7, 60.1, 48.4, 43.5, 36.0, 34.7, 33.9, 33.4, 28.8, 25.0, 24.6, 14.4; MS (ESI) m/z 500 $(M + Na)^+$.

8-Oxo-8-[[2-oxo-2-[(2-phenylethyl)amino]-1-(phenylmethyl)ethyl](phenylmethyl)amino]-octanoic Acid (28). The crude material is purified by column chromatography, using petroleum ether/EtOAc 4:6 (+ formic acid 1%) as eluant to give a white solid (85%). IR (KBr) 3260, 2930, 2350, 1735, 1612, 1454, 1223, 1173, 771, 702 cm^{-1}; ^1H NMR (300 MHz, $CDCl_3$) δ 10.45 (br s, 1-H), 7.29−7.10 (m, 15-H), 6.78 (t, J = 5.8 Hz, 1-H), 5.13 (t, J = 7.7 Hz, 1-H), 4.53 (m, 2-H), 3.41−3.18 (m, 3-H), 3.01 (m, 1-H), 2.66 (m, 2-H), 2.30 (t, J = 7.1 Hz, 2-H), 2.18 (t, J = 7.1 Hz, 2-H), 1.57 (m, 4-H), 1.24 (m, 4-H); ^{13}C NMR (75 MHz, $CDCl_3$) δ 175.7 (2C), 170.3, 139.0, 137.3, 137.2, 129.4, 128.9, 128.8, 128.7, 128.6, 127.5, 126.8, 126.5, 126.2, 59.9, 49.4, 40.6, 35.4, 35.0, 34.1, 33.8, 28.9 (2C), 25.0, 24.7; MS (ESI) m/z 537 $(M + Na)^+$; Mp = 96−98 °C.

8-[Methyl[2-oxo-2-[(2-phenylethyl)amino]-1-(phenylmethyl)ethyl]amino]-8-oxo-octanoic Acid (29). The crude material is purified by column chromatography, using EtOAc as eluant to give a clorless oil (98%). IR (KBr) 2934, 2360, 1718, 1625, 1454, 1259, 1199, 748, 698 cm^{-1}; ^1H NMR (300 MHz, $CDCl_3$) δ 10.45 (br s, 1-H), 7.30−7.05 (m, 10-H), 6.69 (t, J = 5.8 Hz, 1-H), 5.34 (t, J = 7.1 Hz, 1-H), 3.46 (m, 2-H), 3.19 (m, 1-H), 2.91 (m, 1-H), 2.73 (s, 3-H), 2.65 (m, 2-H), 2.27 (m, 2-H), 2.09 (m, 2-H), 1.55 (m, 2-H), 1.36 (m, 2-H), 1.18 (m, 4-H); ^{13}C NMR (75 MHz, $CDCl_3$) δ 177.7, 174.8, 170.2, 138.9, 137.1, 128.9, 128.8, 128.5 (2C), 126.7, 126.4, 57.1, 40.4, 35.4, 34.1, 34.0, 33.5, 31.2, 28.9, 28.8, 24.6, 24.5; MS (ESI) m/z 461 $(M + Na)^+$.

8-[[1-([1,1′-Biphenyl]-4-ylmethyl)-2-oxo-2-[(2-phenylethyl)amino]ethyl](phenylmethyl)amino]-8-oxo-octanoic Acid (30). The crude material is purified by column chromatography, using petroleum ether/EtOAc 3:7 (+ formic acid 1%) as eluant to give an amorphous solid (99%). IR (KBr) 2933, 2359, 1625, 1452, 1361, 1198, 761, 730, 696 cm^{-1}; ^1H NMR (300 MHz, $CDCl_3$) δ 11.05 (br s, 1-H), 7.78−7.11 (m, 19-H), 6.88 (t, J = 5.8 Hz, 1-H), 5.25 (t, J = 7.4 Hz, 1-H), 4.60 (m, 2-H), 3.52−3.29 (m, 3-H), 3.13 (m, 1-H), 2.72 (m, 2-H), 2.35 (t, J = 7.4 Hz, 2-H), 2.24 (t, J = 7.4, 2-H), 1.61 (m, 4-H), 1.29 (m, 4-H); ^{13}C NMR (75 MHz, $CDCl_3$) δ 178.2, 175.8, 170.3, 140.8, 139.6, 139.0, 137.3, 136.5, 129.9, 129.2, 128.9, 128.8, 128.6, 128.4, 127.3, 127.1, 126.5, 126.3, 125.5, 59.9, 49.4, 40.7, 35.5, 34.5, 34.1, 33.9, 29.0 (2C), 25.1, 24.7; MS (ESI) m/z 589 $(M - H)^-$.

8-Oxo-8-[[1-[[(2-phenylethyl)amino]carbonyl]octyl](phenylmethyl)amino]-octanoic Acid (31). The crude material is purified by column chromatography, using petroleum ether/EtOAc 3:7 (+ formic acid 1%) as eluant to give a colorless oil (67%). IR (KBr) 2926, 1717, 1624, 1275, 1085, 764, 698 cm^{-1}; ^1H NMR (300 MHz, $CDCl_3$) δ 7.35−7.08 (m, 10-H), 6.65 (t, J = 5.5 Hz, 1-H), 4.83 (m, 1-H), 4.57 (d, J = 17.8 Hz, 1-H), 4.45 (d, J = 17.8 Hz, 1-H), 3.43 (q, J = 6.6 Hz, 2-H), 2.76 (t, J = 7.1 Hz, 2-H), 2.28 (t, J = 7.4 Hz, 2-H), 2.18 (m, 2-H), 1.85 (m, 1-H), 1.56 (m, 4-H), 1.43 (m, 1-H), 1.30−1.05 (m, 14-H), 0.83 (t, J = 6.6 Hz, 3-H); ^{13}C NMR (75 MHz, $CDCl_3$) δ 178.0, 175.7, 170.9, 139.0, 137.7, 128.8, 128.7, 128.5, 127.3, 126.4, 126.0, 57.8, 48.3, 40.5, 35.5, 34.0, 33.7, 31.8, 29.4, 29.1, 28.9 (2C), 28.5, 26.4, 25.0, 24.7, 22.6, 14.2; MS (ESI) m/z 521 $(M - H)^-$.

General Procedure for the Preparation of Hydroxamic Acids (32−40). The carboxylic acid (1 equiv) is dissolved in dichloromethane and TEA (1 equiv), EDCI (1.1 equiv), and *o*-(*tert*-butyldimethylsilyl)hydroxylamine (1.5 equiv) are added. The reaction is stirred at room temperature for 1 h. The solvent is evaporated. The crude material is diluted with THF and TBAF (1 equiv) in 1 M THF is added. The reaction is stirred at room temperature for 30 min and evaporated. EtOAc is added and the organic phase is washed with 2 N HCl (×3) and with brine (×1), dried over sodium sulfate, and evaporated. The crude material is purified by column chromatography to give the hydroxamic acid.

***N*^{1}-[2-(Cyclohexylamino)-2-oxo-1-(phenylmethyl)ethyl]-*N*^{7}-hydroxy-*N*^{1}-(phenylmethyl)-heptenediamide (32).** The crude material is purified by column chromatography, using EtOAc/MeOH (+ formic acid 1%) as eluant to give an amorphous brown solid (41%, two steps). IR (KBr) 3249, 2929, 2359, 1625, 1451, 1259, 1029, 748, 730 cm^{-1}; ^1H NMR (300 MHz, $CDCl_3$) δ 7.29−7.15 (m, 10-H), 6.19 (d, J = 7.1 Hz, 1-H), 5.00 (t, J = 7.4 Hz, 1-H), 4.65 (m, 1-H), 4.47 (m, 1-H), 3.65 (m, 1-H), 3.16 (m, 1-H), 2.98 (m, 1-H), 2.17 (m, 4-H), 1.70−1.42 (m, 10-H), 1.27−1.00 (m, 6-H); ^{13}C NMR (75 MHz, $CDCl_3$) δ 175.6, 171.2, 169.0, 137.3, 137.1, 129.3, 128.9, 128.6, 127.5, 126.8, 126.2, 60.0, 49.3, 48.3, 35.2, 35.0, 33.4, 32.6, 28.0, 25.5, 24.7 (2C), 24.2; MS (ESI) m/z 516 $(M + Na)^+$.

***N*^{1}-Hydroxy-*N*^{7}-[2-oxo-2-[(2-phenylethyl)amino]-1-(phenylmethyl)ethyl]-*N*^{7}-(2-phenylethyl)-heptanediamide (33).** The crude material is purified by column chromatography, using EtOAc/MeOH 9:1 (+ formic acid 1%) as eluant to give a colorless oil (32%, two steps). IR (KBr) 3232, 1624, 1453, 1178, 1029, 734 cm^{-1}; ^1H NMR (300 MHz, $CDCl_3$) δ 7.37−7.08 (m, 15-H), 6.81 (br t, 1-H), 4.91 (t, J = 7.1 Hz, 1-H), 3.58−3.12 (m, 6-H), 2.89−2.49 (m, 4-H), 2.12 (m, 4-H), 1.53 (m, 4-H), 1.22 (m, 2-H); ^{13}C NMR (75 MHz, $CDCl_3$) δ 174.8, 171,1, 170.1, 138.9, 138.0, 137.4, 129.0, 128.9, 128.8, 128.7, 128.6, 128.5, 127.0, 126.8, 126.5, 52.7, 48.2, 40.7, 35.8, 35.4, 34.7, 33.1, 32.5, 28.4, 25.1, 24.4; MS (ESI) m/z 552 $(M + Na)^+$.

***N*^{1}-Hydroxy-*N*^{7}-[2-oxo-2-[(2-phenylethyl)amino]-1-(phenylmethyl)ethyl]-*N*^{7}-(phenylmethyl)-heptanediamide (34).** The crude material is purified by column chromatography, using EtOAc/MeOH 9:1 as eluant to give an amorphous white solid (36%, two steps). IR (KBr) 3243, 2940, 1627, 1453, 1361, 1029, 909, 728 cm^{-1}; ^1H NMR (300 MHz, $CDCl_3$) δ 7.40−7.01 (m, 15-H), 6.42 (br t, 1-H), 4.99 (t, J = 7.1 Hz, 1-H), 4.53 (d, J = 17.6 Hz, 1-H), 4.38 (d, J = 17.6 Hz, 1-H), 3.48−3.14 (m, 3-H), 2.95 (m, 1-H), 2.61 (m, 2-H), 2.17 (m, 4-H), 1.53 (m, 4-H), 1.22 (m, 2-H); ^{13}C NMR (75 MHz, $CDCl_3$) δ 175.3, 171.3, 170.1, 138.9, 137.3, 137.1, 129.8, 128.9, 128.8, 128.6, 128.5, 127.5, 126.8, 126.5, 126.2, 59.8, 49.3, 40.6, 35.4, 35.0, 33.4, 32.3, 28.1, 24.8, 24.7; MS (ESI) m/z 538 $(M + Na)^+$.

***N*^{1}-[1-[(Cyclohexylamino)carbonyl]heptyl]-*N*^{7}-hydroxy-*N*^{1}-(2-phenylethyl)-heptanediamide (35).** The crude material is purified by column chromatography, using EtOAc/MeOH 9:1 as eluant to give a light brown oil (54%, two steps). IR (KBr) 3252, 2928, 2855, 1623, 1536, 1452, 1251, 1030, 734 cm^{-1}; ^1H NMR (300 MHz, $CDCl_3$) δ 7.35−7.08 (m, 5-H), 6.67 (d, J = 7.7 Hz, 1-H), 4.76 (t, J = 7.4 Hz, 1-H), 3.68 (m, 1-H), 3.44 (m, 2-H), 2.83 (m, 1-H), 2.72 (m, 1-H), 2.29 (m, 2-H), 2.13 (m, 2-H), 2.00−1.52 (m, 12-H), 1.38−1.02 (m, 14-H), 0.80 (t, J = 6.9 Hz, 3-H); ^{13}C NMR (75 MHz, $CDCl_3$) δ 174.8, 171.2, 170.3, 138.2, 128.8, 128.7, 126.8, 57.9, 48.2, 46.9, 36.4, 33.2, 32.8, 32.4, 31.7, 29.1, 28.6, 28.5, 26.2, 25.5, 25.1, 24.8 (2C), 22.6, 14.1; MS (ESI) m/z 524 $(M + Na)^+$.

***N*^{1}-Hydroxy-*N*^{7}-[2-oxo-1-(phenylmethyl)-2-[(phenylmethyl)amino]ethyl]-*N*^{7}-(2-phenylethyl)-heptanediamide (36).** The crude material is purified by column chromatography, using EtOAc as eluant to give an amorphous white solid (50%, two steps). IR (KBr) 3248,

1622, 1453, 1260, 1029, 798, 748 cm^{-1}; ^1H NMR (300 MHz, $CDCl_3$) δ 7.33−7.10 (m, 15-H), 5.03 (t, J = 7.7 Hz, 1-H), 4.37 (m, 2-H), 3.50−3.13 (m, 4-H), 2.64 (m, 2-H), 2.20−2.02 (m, 4-H), 1.47 (m, 4-H), 1.15 (m, 2-H); ^{13}C NMR (75 MHz, $CDCl_3$) δ 174.8, 171.3, 170.5, 138.2, 138.1, 137.2, 129.2, 128.9, 128.7, 128.6 (2C), 127.7, 127.3, 126.8, 126.6, 60.5, 48.1, 43.5, 36.0, 34.8, 33.1, 32.3, 28.2, 25.0, 24.3, 14.2; MS (ESI) m/z 538 $(M + Na)^+$.

N^1-Hydroxy-N^8-[2-oxo-2-[(2-phenylethyl)amino]-1-(phenylmethyl)ethyl]-N^8-(phenylmethyl)-octanediamide (37). The crude material is purified by column chromatography, using EtOAc/MeOH 8:2 as eluant to give a brown oil 36%, two steps). IR (KBr) 3248, 2927, 2360, 1626, 1260, 1075, 1030, 974 cm^{-1}; ^1H NMR (300 MHz, $CDCl_3$) δ 7.32−6.99 (m, 15-H), 6.36 (t, J = 5.5 Hz, 1-H), 4.96 (t, J = 7.7 Hz, 1-H), 4.53 (d, J = 17.6 Hz, 1-H), 4.39 (d, J = 17.6 Hz, 1-H), 3.44−3.13 (m, 3-H), 2.95 (m, 1-H), 2.61 (m, 2-H), 2.17 (t, J = 7.1 Hz, 2-H), 2.07 (t, J = 7.1 Hz, 2-H), 1.53 (m, 4-H), 1.22 (m, 4-H); ^{13}C NMR (75 MHz, $CDCl_3$) δ 175.4, 171.1, 170.1, 138.9, 137.3, 137.3, 129.3, 128.9, 128.8, 128.6 (2C), 127.5, 126.8, 126.5, 126.3, 59.9, 49.5, 40.6, 35.4, 35.0, 33.6, 32.5, 28.4, 28.3, 24.9, 24.8; MS (ESI) m/z 552 $(M + Na)^+$.

N^1-Hydroxy-N^8-methyl-N^8-[2-oxo-2-[(2-phenylethyl)amino]-1-(phenylmethyl)ethyl]-octanediamide (38). The crude material is purified by column chromatography, using EtOAc/MeOH 8:2 as eluant to give a colorless oil (49%, two steps). IR (KBr) 3232, 2931, 1626, 1530, 1454, 1260, 1084, 748, 665 cm^{-1}; ^1H NMR (300 MHz, $CDCl_3$) δ 7.33−7.08 (m, 10-H), 6.49 (br t, 1-H), 5.30 (t, J = 6.9 Hz, 1-H), 3.43 (m, 2-H), 3.21 (m, 1-H), 2.91 (m, 1-H), 2.74 (s, 3-H), 2.65 (m, 2-H), 2.10 (m, 4-H), 1.57 (quint, J = 6.9 Hz, 2-H), 1.38 (quint, J = 6.9 Hz, 2-H), 1.18 (m, 4-H); ^{13}C NMR (75 MHz, $CDCl_3$) δ 174.7, 171.2, 170.1, 138.9, 137.2, 128.9, 128.8, 128.5 (2C), 126.7, 126.5, 57.3, 40.5, 35.5, 34.1, 33.4, 32.6, 31.3, 28.5, 28.4, 25.0, 24.4; MS (ESI) m/z 476 $(M + Na)^+$.

N^1-[1-([1,1′-Biphenyl]-4-ylmethyl)-2-oxo-2-[(2-phenylethyl)amino]ethyl]-N^8-hydroxy-N^1-(phenylmethyl)-octanediamide (39). The crude material is purified by column chromatography, using EtOAc/MeOH 9:1 as eluant to give a white solid (65%, two steps). IR (KBr) 3244, 3027, 2930, 2360, 1654, 1361, 1077, 830, 762, 698 cm^{-1}; ^1H NMR (300 MHz, $CDCl_3$) δ 7.60−7.00 (m, 19-H), 6.51 (br t, 1-H), 5.02 (t, J = 7.1 Hz, 1-H), 4.48 (m, 2-H), 3.42−3.15 (m, 3-H), 2.99 (m, 1-H), 2.63 (m, 2-H), 2.17 (t, J = 6.9 Hz, 2-H), 2.04 (m, 2-H), 1.53 (m, 4-H), 1.22 (m, 4-H); ^{13}C NMR (75 MHz, $CDCl_3$) δ 175.5, 171.2, 170.1, 140.8, 139.5, 138.9, 137.2, 136.4, 129.7, 128.9 (2C), 128.8, 128.6, 127.5, 127.3, 127.2, 126.9, 126.5, 126.3, 59.8, 49.4, 40.6, 35.4, 34.7, 33.7, 32.6, 28.5 (2C), 25.0, 24.9; MS (ESI) m/z 628 $(M + Na)^+$; Mp = 58−60 °C.

N^1-Hydroxy-N^8-[1-[[(2-phenylethyl)amino]carbonyl]octyl]-N^8-(phenylmethyl)-octanediamide (40). The crude material is purified by column chromatography, using EtOAc/MeOH 9:1 as eluant to give a colorless oil (40%, two steps). IR (KBr) 3269, 2926, 2856, 1625, 1453, 1417, 1199, 1029, 975 cm^{-1}; ^1H NMR (300 MHz, $CDCl_3$) δ 7.30−7.18 (m, 10-H), 6.66 (br t, 1-H), 4.80 (m, 1-H), 4.53 (m, 4-H), 3.42 (m, 2-H), 2.76 (t, J = 6.9 Hz, 2-H), 2.17 (t, J = 7.1 Hz, 2-H), 2.09 (t, J = 6.9, 2-H), 1.83 (m, 1-H), 1.56 (m, 5-H), 1.30−1.05 (m, 14-H), 0.82 (t, J = 6.6 Hz, 3-H); ^{13}C NMR (75 MHz, $CDCl_3$) δ 175.7, 171.2, 170.9, 138.9, 137.7, 128.8, 128.6, 128.3, 127.5, 126.4, 125.9, 57.9, 48.5, 40.5, 35.5, 33.6, 32.6, 31.7, 29.4, 29.1, 28.9, 28.7, 28.5, 26.4, 25.0, 24.9, 22.6, 14.2; MS (ESI) m/z 536 $(M - H)^-$.

General Procedure for the Preparation of Benzamides (41, 42). The carboxylic acid (1.5 equiv) is dissolved in THF and DCC (1 equiv) and *o*-phenylenediamine (1 equiv) are added. After 12 h, other DCC (1 equiv) is added. The reaction is stirred at room temperature for 24 h. The solvent is evaporated. The crude material is diluted with EtOAc and washed with sat. aq. Na_2CO_3 (×2) and brine (×1), dried over sodium sulfate, evaporated, and purified by column cromatography to give the benzamide.

N^1-(2-Aminophenyl)-N^7-[2-(cyclohexylamino)-2-oxo-1-(phenylmethyl)ethyl]-N^7-(phenylmethyl)-heptanediamide (41). The crude material is purified by column chromatography, using petroleum ether/EtOAc 3:7 as eluant to give a yellow oil (23%). IR (KBr) 3298, 2925, 1630, 1525, 1452, 1300, 1079, 747, 665 cm^{-1}; ^1H NMR (300 MHz, $CDCl_3$) δ 7.40−6.68 (m, 14-H), 6.11 (d, J = 8.0 Hz, 1-H), 4.99 (t, J = 8.0 Hz, 1-H), 4.64 (d, J = 17.6 Hz, 1-H), 4.48 (d, J = 17.6 Hz, 1-H), 3.57 (m, 1-H), 3.16 (m, 1-H), 2.95 (m, 1-H), 2.36 (t, J = 7.4 Hz, 2-H), 2.21 (t, J = 7.4 Hz, 2-H), 1.88−1.47 (m, 10-H), 1.34−1.15 (m, 6-H); ^{13}C NMR (75 MHz, $CDCl_3$) δ 175.2, 169.0 (2C), 140.9, 137.5 (2C), 129.3, 128.9, 128.8, 128.6, 127.4, 127.1, 126.7, 126.2, 125.1, 119.6, 118.3, 60.2, 49.4, 48.1, 36.6, 35.0, 32.7, 28.5, 25.5, 25.4, 24.7 (2C); MS (ESI) m/z 501 $(M + Na)^+$.

N^1-(2-Aminophenyl)-N^8-[1-([1,1′-biphenyl]-4-ylmethyl)-2-oxo-2-[(2-phenylethyl)amino]ethyl]-N^8-(phenylmethyl)-octanediamide (42). The crude material is purified by column chromatography, using petroleum ether/EtOAc 3:7 as eluant to give a brown solid (24%, two steps). IR (KBr) 3289, 2931, 1654, 1524, 1453, 1308, 761, 748, 697 cm^{-1}; ^1H NMR (300 MHz, $CDCl_3$) δ 7.53−6.67 (m, 23-H), 6.38 (br t, 1-H), 5.02 (t, J = 7.1 Hz, 1-H), 4.48 (m, 2-H), 3.42−3.20 (m, 3-H), 3.02 (m, 1-H), 2.67 (m, 2-H), 2.30 (br t, 2-H), 2.18 (br t, 2-H), 1.60 (m, 4-H), 1.24 (m, 4-H); ^{13}C NMR (75 MHz, $CDCl_3$) δ 175.3, 172.0, 170.1, 140.9, 140.8, 139.5, 138.8, 137.3, 136.5, 129.7, 128.9, 128.8 (2C), 128.6, 127.5, 127.3, 127.2, 127.1, 127.0 (2C), 126.9, 126.5, 126.2, 125.4, 124.5, 59.9, 49.4, 40.5, 36.6, 35.5, 34.6, 33.7, 28.8, 28.7, 25.5, 24.9; MS (ESI) m/z 681 $(M + H)^+$; Mp = 62−64 °C (dec).

Biology. Cell Culture, Viability, and HDAC Assay. SH-SY 5Y (neuroblastoma) cells were cultured in MEM (Sigma) supplemented with 10% FBS (fetal bovine serum), 2 mM glutamine, 10 U/mL penicillin, and 100 μg/mL streptomycin. Cells were maintained in a humidified incubator supplied with 5% CO_2/95% air at 37 °C. Cells were subcultured as needed by detaching the cells with 0.25% trypsin and 5 mM EDTA. To analyze cell viability, the colorimetric MTT (3-(4,5-dimethylthiazol-2-yl)-2,5-diphenyltetrazolium bromide) assay was used. Briefly, cells were plated in 24-well plates and treated as indicated for the appropriate time. Compounds or vehicle were added to the cells to give a final DMSO concentration no greater than 0.5%. Cells were washed once in Locke Buffer and 300 μL of MTT (250 μg/mL in Locke Buffer) was added before returning the cells to the incubator for 1 h to allow the formation of the purple formazan crystals. After 1 h, 600 μL isopropanol/0.1 M HCl was added to each well and the absorbance was read at 570 nm in a plate reader (Victor3V, Perkin-Elmer).

For HDAC assays, the HDAC Fluorimetric Cellular Activity Assay (Biomol) was used according to the manufacturer's instructions.

Flow-Cytometric Analysis of Cell-Cycle Status. SHSY5Y grown in the presence or absence of compounds for 16 h were washed once in PBS and resuspended in 1 mL of 30:70 ice cold PBS/EtOH and stored at −20 °C. Cells were then washed twice in PBS and resuspended in PBS containing RNase (100 μg/mL) for 1 h at 37 °C. DNA was then stained with a PBS solution containing 5 mM EDTA and 100 μg/mL propidium iodide for 30 min at 4 °C in the dark. Cell cycle analysis was determined with a FACSVantage SE DiVa (Becton Dickinson).

Molecular Docking Studies. We performed molecular docking calculations on a two dual-core Intel Xeon 3.4 GHz, using Autodock 3.0.5 software.[10] For HDLP metallic center, we considered a nonbonded model according to the nonbonded Zn parameters of Stote[12] (zinc radius = 1.10 Å, well depth = 0.25 kcal/mol). To have an accurate weight of the electrostatics, we derived the partial charge of Zn = 1.175 and of the aminoacids involved in the catalytic center (A169, H170, D168, D258) by DFT calculations B3LYP level by the 6-31G(d) basis set and ChelpG[13] method for population analysis (Gaussian 03 Package software).[14] The charges of the ligands were optimized at DFT level using the B3LYP functional and the 6-31G+(d) basis set, as implemented in Gaussian 03 Package software.[14] For all the docking studies, a grid box size of 66 × 64 × 48 with spacing of 0.375 Å between the grid points and centered at 49.75 (x), 5.0 (y), and 101.491 (z) covering the four hydrophobic pockets (A−D) on the HDLP surface was used. For all the docked structures, all bonds were treated as active torsional bonds. To achieve a representative conformational space during the docking calculations, 10 calculations consisting of 256

runs were performed, obtaining 2560 structures (256 × 10). The Lamarckian genetic algorithm was used for dockings. An initial population of 450 randomly placed individuals, a maximum number of 10.0×10^6 energy evaluations, and a maximum number of 8.0×10^6 generations were taken into account. A mutation rate of 0.02 and a crossover rate of 0.8 were used. Results differing by less than 2.5 Å in positional root-mean-square deviation (rmsd) were clustered together and represented by the result with the inhibition constant (K_i). All the 3D models were depicted using the Python software:[15] molecular surfaces are rendered using Maximal Speed Molecular Surface (MSM).[16]

Acknowledgment. Financial support from Regione Piemonte (Ricerca Sanitaria Finalizzata 2008 to TP, and Ricerca Applicata 2004 to AAG), and M.I.U.R. PRIN 2006 Italy are gratefully acknowledged.

Supporting Information Available: Elemental analysis of all target compounds. This material is available free of charge via the Internet at http://pubs.acs.org.

References

(1) (a) Yoo, C. B.; Jones, P. A. Epigenetic therapy of cancer: past, present and future. *Nat. Rev. Drug Discovery* **2006**, *5*, 37–50. (b) Bolden, J.; Peart, M. J.; Johnstone, R. W. Anticancer activities of histone deacetylases inhibitors. *Nat. Rev. Drug Discovery* **2006**, *5*, 769–784.

(2) (a) Miller, T. A.; Witter, D. J.; Belvedere, S. Histone deacetylases inhibitors. *J. Med. Chem.* **2003**, *46*, 5097–5116. (b) Paris, M.; Porcelloni, M.; Binaschi, M.; Fattori, D. Histone deacetylases inhibitors: from bench to clinic. *J. Med. Chem.* **2008**, *51*, 1505–1529.

(3) Marks, P. A.; Breslow, R. Dimethyl sulfoxide to vorinostat: development of this histone deacetylase inhibitor as an anticancer drug. *Nat. Biotechnol.* **2007**, *25*, 84–90.

(4) Finnin, M. S.; Donigian, J. R.; Cohen, A.; Richon, V. M.; Rifkind, R. A.; Marks, P. A.; Breslow, R.; Pavletich, N. P. Structures of a histone deacetylase homologue bound to the TSA and SAHA inhibitors. *Nature (London)* **1999**, *401*, 188–193.

(5) (a) Furumai, R.; Komatsu, Y.; Nishino, N.; Khochbin, S.; Yoshida, M.; Horinouchi, S. Potent histone deacetylase inhibitors built from trichostatin A and cyclic tetrapeptide antibiotics including trapoxin. *Proc. Natl. Acad. Sci. U.S.A.* **2001**, *98*, 87–92. (b) Yoshida, M.; Furumai, R.; Nishiyama, M.; Komatsu, Y.; Nishino, N.; Horinouchi, S. Histone deacetylase as a new target for cancer chemotherapy. *Cancer Chemother. Pharmacol.* **2001**, *48*, 20–26.

(6) Komatsu, Y.; Tomizaki, K.; Tsukamoto, M.; Kato, T.; Nishino, N.; Sato, S.; Yamori, T.; Tsuruo, T.; Furumai, R.; Yoshida, M.; Horinouchi, S.; Hayashi, H. Cyclic hydroxamic-acid-containing peptide 31, a potent synthetic histone deacetylase inhibitor with antitumor activity. *Cancer Res.* **2001**, *61*, 4459–4466.

(7) (a) Ugi, I.; Meyr, R.; Fetzer, U.; Steinbruckner, C. Versuche mit Isonitrilen. *Angew. Chem., Int. Ed. Engl.* **1959**, *71*, 386–388. (b) Dömling, A.; Ugi, I. Multicomponent reactions with isocyanides. *Angew. Chem., Int. Ed. Engl.* **2000**, *39*, 3168–3210.

(8) (a) Condorelli, F.; Gnemmi, I.; Vallario, A.; Genazzani, A. A.; Canonico, P. L. Inhibitors of histone deacetylase (HDAC) restore the p53 pathway in neuroblastoma cells. *Br. J. Pharmacol.* **2008**, *153*, 657–668. (b) Pirali, T.; Pagliai, F.; Mercurio, C.; Boggio, R.; Canonico, P. L.; Sorba, G.; Tron, G. C.; Genazzani, A. A. Triazole-modified histone deacetylase inhibitors as a rapid route to drug discovery. *J. Comb. Chem.* **2008**, *10*, 624–627.

(9) Mühlethaler-Mottet, A.; Meier, R.; Flahaut, M.; Bourloud, K. B.; Nardou, K.; Joseph, J. M. Complex molecular mechanisms cooperate to mediate histone deacetylase inhibitors anti-tumour activity in neuroblastoma cells. *Mol. Cancer* **2008**, *7*, 55.

(10) Morris, G. M.; Goodsell, D. S.; Halliday, R. S.; Huey, R.; Hart, W. E.; Belew, R. K.; Olson, A. J. Automated docking using a lamarckian genetic algorithm and an empirical binding free energy function. *J. Comput. Chem.* **1998**, *19*, 1639–1662.

(11) (a) Wang, D.-F.; Wiest, O.; Helquist, P.; Lan-Hargest, H.-Y.; Wiech, N. L. On the function of the 14 Å long internal cavity of histone deacetylase-like protein: implications for the design of histone deacetylase inhibitors. *J. Med. Chem.* **2004**, *47*, 3409–3417. (b) Park, H.; Lee, S. Homology modeling, force field design, and free energy simulation studies to optimize the activities of histone deacetylase inhibitors. *J. Comput.-Aided Mol. Des.* **2004**, *18*, 375–388. (c) Wang, D.-F.; Helquist, P.; Wiech, N. L.; Wiest, O. Toward selective histone deacetylase inhibitor design: homology modeling, docking studies, and molecular dynamics simulations of human class I histone deacetylases. *J. Med. Chem.* **2005**, *48*, 6936–6947. (d) Maulucci, N.; Chini, M. G.; Di Micco, S.; Izzo, I.; Cafaro, E.; Russo, A.; Gallinari, P.; Paolini, C.; Nardi, M. C.; Casapullo, A.; Riccio, R.; Bifulco, G.; De Riccardis, F. Molecular insights into azumamide E histone deacetylases inhibitory activity. *J. Am. Chem. Soc.* **2007**, *129*, 3007–3012. (e) Di Micco, S.; Terracciano, S.; Bruno, I.; Rodriquez, M.; Riccio, R.; Taddei, M.; Bifulco, G. Molecular modeling studies toward the structural optimization of new cyclopeptide-based HDAC inhibitors modelled on the natural product FR235222. *Bioorg. Med. Chem.* **2008**, *16*, 8635–8642.

(12) Stote, R. H.; Karplus, M. Zinc binding in proteins and solution: a simple but accurate nonbonded representation. *Proteins* **1995**, *23*, 12–31.

(13) Breneman, C. M.; Wiberg, K. B. Determining atom-centered monopoles from molecular electrostatic potentials. The need for high sampling density in formamide conformational analysis. *J. Comput. Chem.* **1990**, *11*, 361–373.

(14) Frisch, M. J.; Trucks, G. W.; Schlegel, H. B.; Scuseria, G. E.; Robb, M. A.; Cheeseman, J. R.; Montgomery, J. A., Jr.; Vreven, T.; Kudin, K. N.; Burant, J. C.; Millam, J. M.; Iyengar, S. S.; Tomasi, J.; Barone, V.; Mennucci, B.; Cossi, M.; Scalmani, G.; Rega, N.; Petersson, G. A.; Nakatsuji, H.; Hada, M.; Ehara, M.; Toyota, K.; Fukuda, R.; Hasegawa, J.; Ishida, M.; Nakajima, T.; Honda, Y.; Kitao, O.; Nakai, H.; Klene, M.; Li, X.; Knox, J. E.; Hratchian, H. P.; Cross, J. B.; Bakken, V.; Adamo, C.; Jaramillo, J.; Gomperts, R.; Stratmann, R. E.; Yazyev, O.; Austin, A. J.; Cammi, R.; Pomelli, C.; Ochterski, J. W.; Ayala, P. Y.; Morokuma, K.; Voth, G. A.; Salvador, P.; Dannenberg, J. J.; Zakrzewski, V. G.; Dapprich, S.; Daniels, A. D.; Strain, M. C.; Farkas, O.; Malick, D. K.; Rabuck, A. D.; Raghavachari, K.; Foresman, J. B.; Ortiz, J. V.; Cui, Q.; Baboul, A. G.; Clifford, S.; Cioslowski, J.; Stefanov, B. B.; Liu, G.; Liashenko, A.; Piskorz, P.; Komaromi, I.; Martin, R. L.; Fox, D. J.; Keith, T.; Al-Laham, M. A.; Peng, C. Y.; Nanayakkara, A.; Challacombe, M.; Gill, P. M. W.; Johnson, B.; Chen, W.; Wong, M. W.; Gonzalez, C.; Pople, J. A. *Gaussian 03*, revision E.01; Gaussian, Inc.: Wallingford, CT, 2004.

(15) Sanner, M. F. Python: a programming language for software integration and development. *J. Mol. Graphics Modell.* **1999**, *17*, 57–61.

(16) Sanner, M. F.; Olson, A. J.; Spehner, J. C. Reduced surface: an efficient way to compute molecular surfaces. *Biopolymers* **1996**, *38*, 305–320.

JM801529C